Electronic Supplementary Material (ESI) for Nanoscale.
This journal is © The Royal Society of Chemistry 2016

Supporting Information for

New type high-index dielectric nanosensors based on scattering intensity shift

Jiahao Yan, Pu Liu, Zhaoyong Lin & Guowei Yang *

State Key Laboratory of Optoelectronic Materials and Technologies, Nanotechnology Research Center, School of Materials Science & Engineering, School of Physics & Engineering, Sun Yat-sen University, Guangzhou 510275, Guangdong, P. R. China.

*Corresponding author: stsygw@mail.sysu.edu.cn

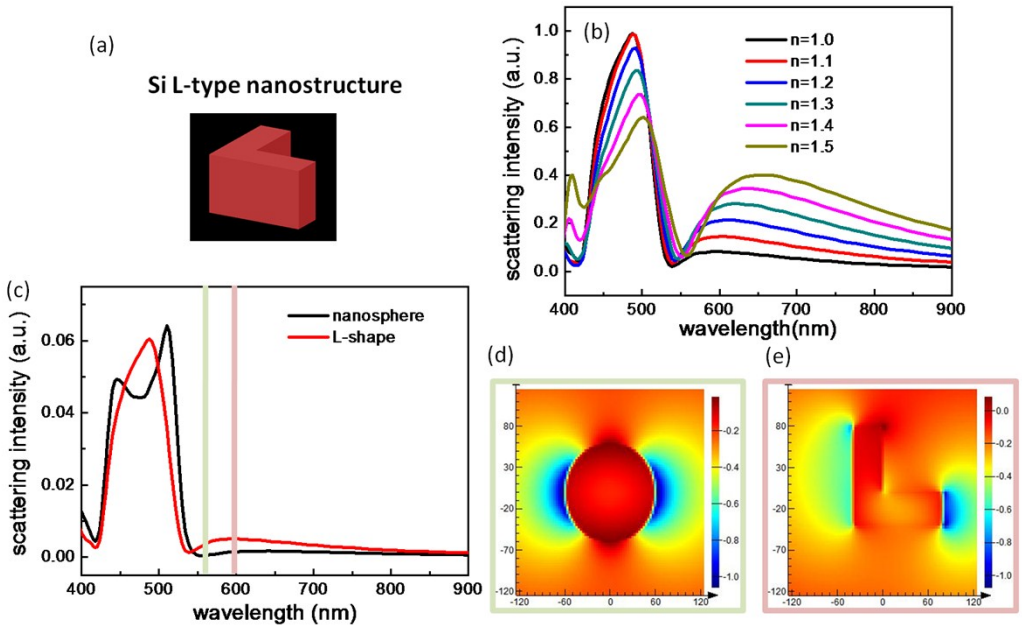

Figure S1. Scattering spectra of a L-shape silicon nanostructure under different ambient refractive indexes. (a) Schematic shows the L-type Si nanostructure. (b) The backward scattering spectra under different ambient refractivities. (c) Comparison between L-shape nanostructures and nanospheres. (d) (e) Electric field distributions of nanosphere and L-shape nanostructure when the field enhancement factors are equal. Their locations in spectra are revealed by vertical bar in (c).

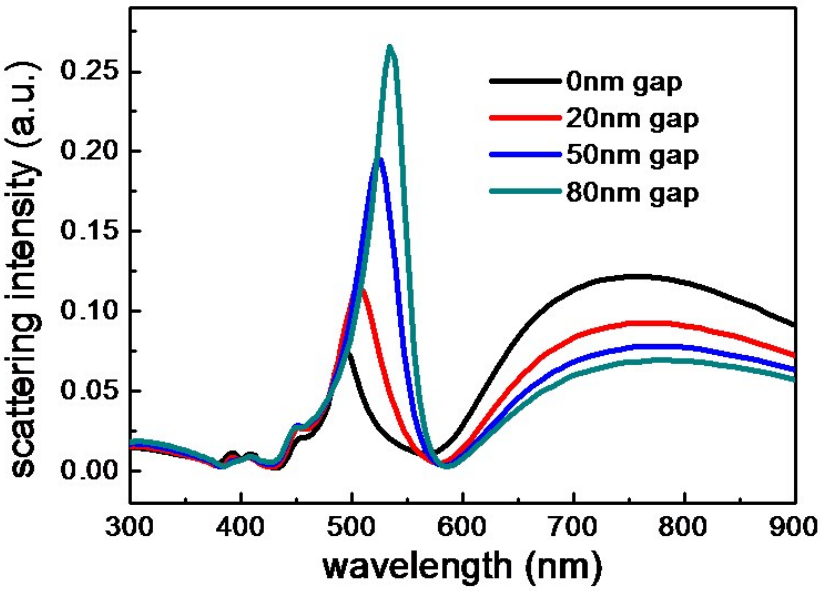

Figure S2. Calculated backward scattering spectra of silicon nanosphere dimers with different gap distances.

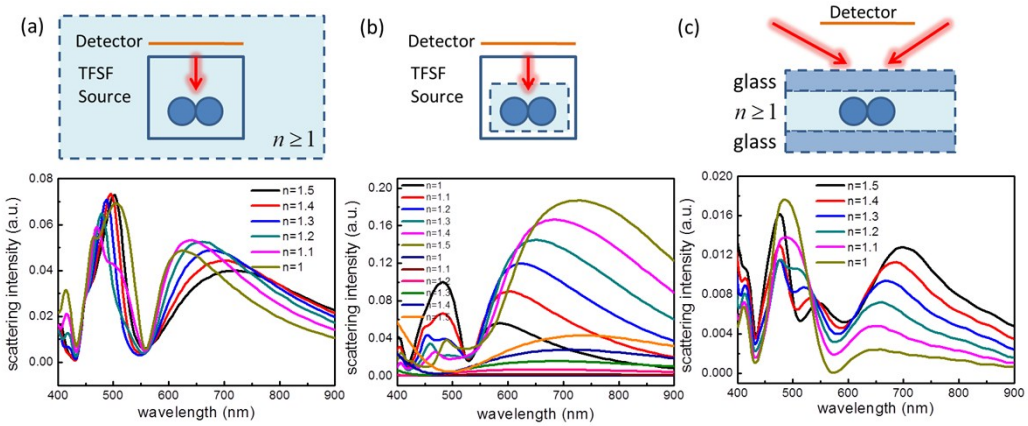

Figure S3. Comparison between different simulated methods. (a)The scattering spectra of silicon nanosphere dimer under different ambient refractive index through setting background refractive index. (b) Scattering spectra of silicon dimer under different ambient refractive index through wrapping nanostructures with cubes with desirable refractive indexes. And scattering spectra near the bottom are the scattering from pure cube, which exclude the obvious intensity changes arise from the scattering from cube. (c) Simulated scattering spectra under 53°C oblique incidence on fluid filled thin layer sandwiched between glasses, which is similar to the situation in experiment.

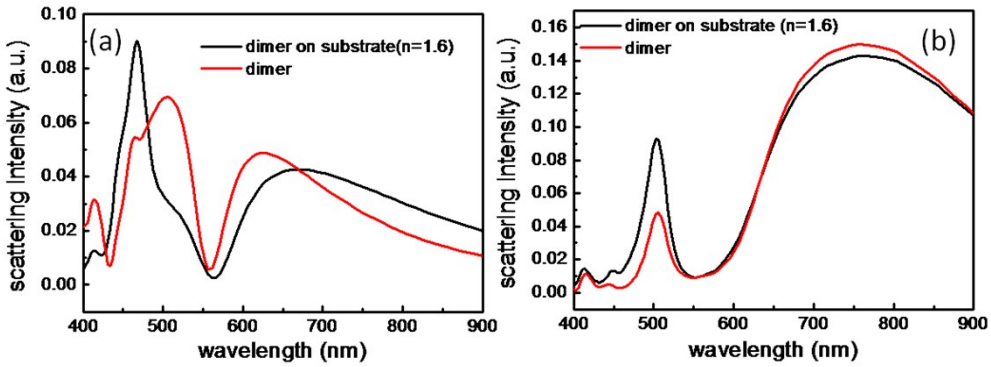

Figure S4. The influences of ITO substrates (n=1.6) on scattering behaviors of a silicon dimer with diameter of 130 nm in air (a) and in solution (n=1.5; b)

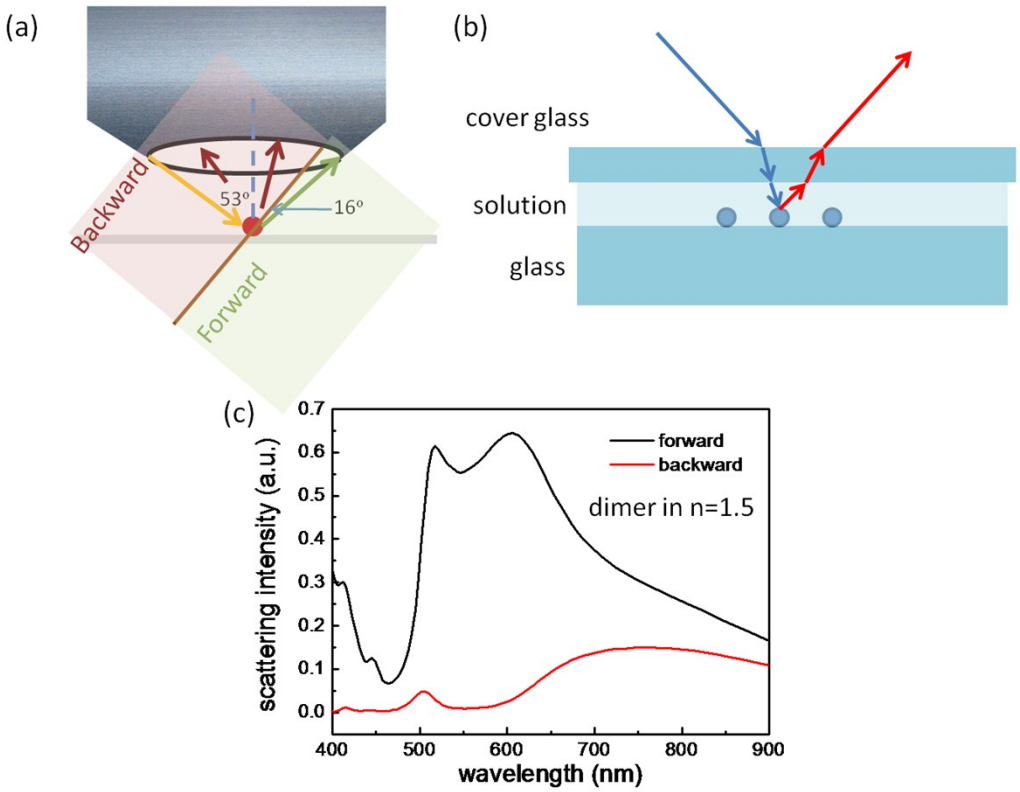

Figure S5. The influences of oblique incidence on scattering behaviors. (a) Schematic shows the oblique incidence (53°; orange arrow) and the ratio between backward and forward scattering collected by dark-field objective. (b) Schematic shows the refraction occurred between solution and cover glass, cover glass and air. (c) Forward and backward scattering from a typical silicon dimer with diameter of 130 nm in ambient refractivity of 1.5.

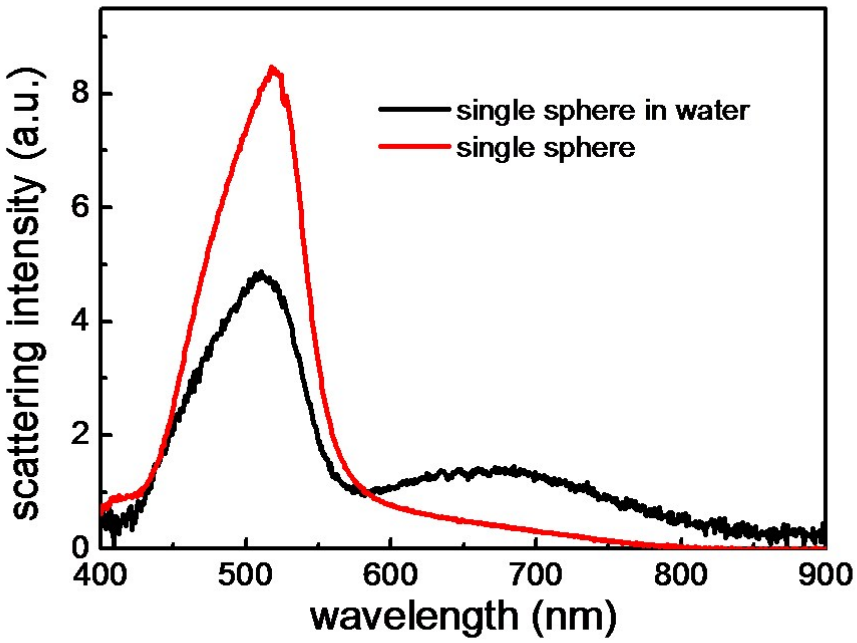

Figure S6. Measured backward scattering spectra of a single silicon nanosphere in air (n=1) and in water (n=1.33).

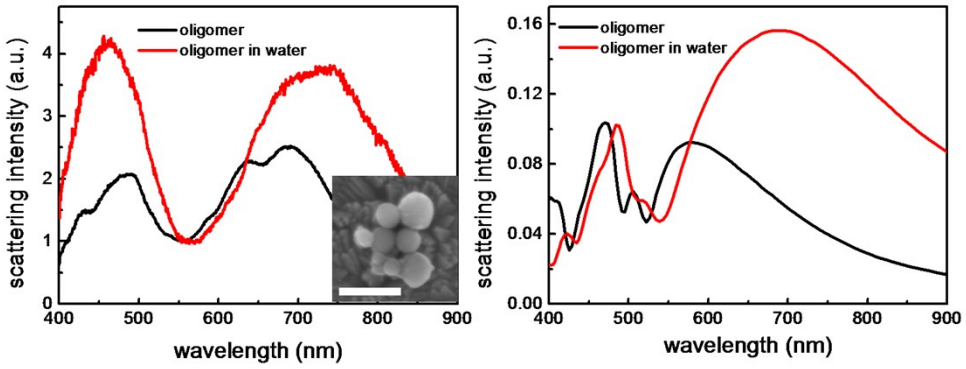

Figure S7. Measured scattering spectra of a typical silicon oligomer (left) in air (n=1) and in water (n=1.33). Inset is the corresponding SEM image. The scale bar is 100nm. Calculated scattering spectra of this oligomer (right) in air and in water.

Table S1. The comparison between the sensitivity of silicon dimer and sensitivities of other plasmonic sensors.

Nanostructures	Sensitivity (nm, eV or a.u. per RIU)	FWHM or SDSI(standard deviation of scattering intensity)	FOM	Ideal resolution	Sensitivity(counts)
Ag nanocubes[1]	1.3eV	0.065eV	20	0.0003eV	4333
Au nanorings[2]	380nm	23nm	16.5	0.08nm	4750
Au nanocavities[3]	405nm	19nm	21	0.08nm	5063
Au nanobipyramids[4]	540nm	120nm	5.4	0.08nm	6750
Au nanoframes[5]	620nm			0.08nm	7750
AuNP@SiO2 particles[6]	737nm			0.08nm	9213
Au nanorings[7]	880nm	440nm	2	0.08nm	11000
Au mushroom arrays[8]	1010nm	10nm	108	0.08nm	12625
Ag annular cavity arrays[9]	1505nm	18nm	85	0.08nm	18813
Au split-ring resonators[10]	3366nm	521nm	6.5	0.08nm	42075
Si nanosphere dimer	11.68	0.1	116.8	0.00001	1168000

References:

1. Zhang, S., Bao, K., Halas, N. J., Xu, H. & Nordlander, P. Substrate-induced Fano resonances of a plasmonic nanocube: a route to increased-sensitivity localized surface plasmon resonance sensors revealed. *Nano Lett.* **11**, 1657-1663 (2011).

2. Lodewijks, K., Van Roy, W., Borghs, G., Lagae, L. & Van Dorpe, P. Boosting the figure-of-merit of LSPR-based refractive index sensing by phase-sensitive measurements. *Nano Lett.* **12**, 1655-1659 (2012).

3. Cattoni, A. *et al.* $\lambda^3/1000$ Plasmonic nanocavities for biosensing fabricated by soft UV nanoimprint lithography. *Nano Lett.* **11**, 3557-3563 (2011).

4. Chen, H., Kou, X., Yang, Z., Ni, W. & Wang, J. Shape- and size-dependent refractive index sensitivity of gold nanoparticles. *Langmuir* **24**, 5233-5237 (2008).

5. Mahmoud, M. A. & El-Sayed, M. A. Gold Nanoframes: Very High Surface Plasmon Fields and Excellent Near-Infrared Sensors. *J. Am. Chem. Soc.* **132**, 12704-12710 (2010).

6.Banholzer, M. J., Harris, N., Millstone, J. E., Schatz, G. C. & Mirkin, C. A. Abnormally large plasmonic shifts in silica-protected gold triangular nanoprisms. *J. Phys. Chem. C* **114**, 7521-7526 (2010).

7. Larsson, E. M., Alegret, J., Käll, M. & Sutherland, D. S. Sensing characteristics of NIR localized surface plasmon resonances in gold nanorings for application as ultrasensitive biosensors. *Nano Lett.* **7**, 1256-1263 (2007).

8.Shen, Y. *et al.* Plasmonic gold mushroom arrays with refractive index sensing figures of merit approaching the theoretical limit. *Nat. Commun.* **4**, 2381 (2013).

9.Ni, H., Wang, M., Shen, T. & Zhou, J. Self-assembled large-area annular cavity arrays with tunable cylindrical surface plasmons for sensing. *ACS Nano* **9**, 1913-1925 (2015).

10. Pryce, I. M., Kelaita, Y. A., Aydin, K. & Atwater, H. A. Compliant metamaterials for resonantly enhanced infrared absorption spectroscopy and refractive index sensing. *ACS Nano* **5**, 8167-8174 (2011).